EduChemia
Jurnal Kimia dan Pendidikan

Vol.10, No.1, 2024, p. 85-96
e-ISSN 2502-4787

STRUCTURE AND PROPERTIES OF α-Fe_2O_3 BASED ON NATURAL IRON SAND THROUGH A LOW-TEMPERATURE PROCESS AS AN ADSORBENT OF METAL ION Mn

Wiwik Indrawati[1], Silviana Simbolon[2*], Mochammad Rizky Apadi[2], Kusdi Prijono[3], Edo Prasetyo Nugroho[4], Muhammad Yunus[2,5]

[1] *Chemical Engineering, Universitas Pamulang, Tangerang Selatan,15417, Indonesia;*
[2] *Mechanical Engineering, Universitas Pamulang, Tangerang Selatan,15417, Indonesia;*
[3]*Directorate of Laboratory Management, Research Facilities, and Science and Technology Areas, BRIN, Tangerang Selatan, 15314, Indonesia;*
[4]*Research Centre for Advance Materials, BRIN, Tangerang Selatan, 15314, Indonesia;*
[5]*Research Centre for Nuclear Reactor Technology, BRIN, Tangerang Selatan, 15314, Indonesia;*

*Corresponding author: dosen01923@unpam.ac.id

Received: 09 Januari 2025. Accepted: 20 Mei 2025. Published: 22 Juni 2025

DOI: 10.30870/educhemia.v10i1.30761

Abstract: One of the countermeasures against heavy metal environmental pollution is through an adsorption process utilizing nanoparticle technology, one of which uses hematite (α-Fe_2O_3) nanoparticles. In this study, the manufacture of α-Fe_2O_3 nanoparticles derived from natural iron sand through the process of precipitation as adsorbent of the heavy metal manganese (Mn) was carried out. The variable used is the temperature of the coprecipitation process in the range of 60–80°C. Furthermore, characterization and adsorptivity tests of α-Fe_2O_3 nanoparticles against the heavy metal ion Mn were carried out. The synthesized α-Fe_2O_3 was characterized in terms of phase using XRD, morphological structure using SEM–EDS, density using pycnometer and adsorption using AAS. The results obtained from XRD show that α-Fe_2O_3 crystallizes well in the (104) plane at the 2θ region of 35.612° and has the smallest crystal diameter of 3.03760 nm at 60°C. SEM revealed that there was still agglomeration in the results and a particle size distribution of 62 nm at 60°C. The density results revealed the highest value at 80°C, with a value of 30 g/cm^3. However, the manganese (Mn) adsorption results revealed the optimal conditions for the value of the Mn content adsorbed at 70°C, namely, 2176 μ/g.

Keywords: Nanoparticles, Hematite, Adsorption, Coprecipitation.

Abstract: alah satu penyelesaian terhadap polusi logam berat pada lingkungan yaitu melalui proses adsorpsi menggunakan teknologi nanopartikel, salah satunya dengan nanopartikel hematit α-Fe2O3. Dalam penelitian ini, pembuatan α-Fe2O3 dari pasir besi alami melalui proses presipitasi sebagai adsorben logam berat mangan (Mn) telah dilakukan. Variabel yang digunakan yaitu temperatur proses kopresipitasi yaitu pada rentang 60-80 °C. Selanjutnya, karakterisasi dan tes adsorptivitas dari nanopartikel α-Fe2O3 untuk ion logam berat Mn dilakukan. Produk hematit α-Fe_2O_3 hasil sintesis dikarakterisasi fasenya menggunakan XRD, diidentifikasi struktur morfologi menggunakan SEM-EDS, ditentukan densitasnya menggunakan piknometer dan diuji adsorptivitasnya menggunakan AAS. Hasil yang diperoleh dari XRD menunjukan bahwa α-Fe_2O_3 terkristalisasi baik pada bidang (104) dengan daerah 2θ yaitu pada 35.612°, dan memiliki ukuran diameter kristal terkecil yaitu 3.03760 nm pada 60 °C. Hasil pencitraan SEM menunjukkan bahwa masih terdapat aglomerasi pada produk dan diperoleh distribusi ukuran partikel 62 nm pada 60 °C. Ukuran densitas yang diperoleh pada nilai tertinggi 30 gr/cm3 yaitu pada 80 °C. Hasil adsorpsi Mn menunjukkan kondisi optimal diperoleh pada pada suhu 70 °C dengan kandungan Mn teradsorp yaitu 2176 µ/g.

Kata kunci: nanopartikel, hematit, adsorpsi, kopresipitasi

INTRODUCTION

Owing to rapid industrialization, water contamination is becoming a more serious problem globally. According to prediction statistics, more than 1000 million people living in arid regions will face a scarcity of clean water by 2025. Among the various hazardous pollutants in water, heavy metal ions such as Hg^{2+}, Cd^{2+}, Pb^{2+}, Mn^{2+}, and Zn^{2+} have attracted much attention because of their well-known toxic properties and resistance to direct biological treatment. These metal ion wastes originate from fossil fuel combustion and waste disposal from various industries, such as chemical manufacturing, smelting, electroplating, textiles, alloy manufacturing, and lead storage batteries (Huang et al., 2019; Jiang et al., 2014; Rezaei et al., 2021; Yi et al., 2017). In fact, metals are important for the physiochemical functions of our body, and the concentration of these metal ions has a great influence on the body. If the amount of these ions is greater than that required by the biological system, it will be fatal and a source of interference with the normal biological processes occurring in the body. In particular, excess Mn ions can cause neurotoxicity, heart attack, vascular disorders, and liver cancer in the body (Brzóska et al., 2022; Riseberg et al., 2022).

Hematite (α-Fe_2O_3) is a more thermodynamically stable mineral than various other types of iron oxide in the presence of oxygen and exhibits strong electron–electron interactions and electron–photon resonance accompanied by a complex electronic structure with interesting optoelectronic characteristics (Al-Hakkani et al., 2021). In general, α-Fe_2O_3 nanoparticles can be used in photocatalysts, gas sensors, lithium-ion batteries, photoelectrochemical cells, and humidity sensors because of their high corrosion resistance and ability to serve as semiconductors [8]. For some applications in the field of biomaterials, α-Fe_2O_3 nanoparticles are used for cellular labeling/cell separation detoxification of biological fluids, tissue repair, drug delivery, magnetic resonance imaging, hyperthermia (heat) in the treatment of malignant tumors, cytotoxicity, and antibacterial and UV protection and have been considered for a variety of uses in various fields because they are nontoxic and environmentally safe and are almost unaffected by oxidation changes (Gulzar et al., 2022; Ikram et al., 2022; Lassoued et al., 2017a). Currently, synthesized α-Fe_2O_3 nanoparticles have also been widely used as catalysts or adsorbent agents to minimize or remove highly toxic materials such as dyes, pharmaceuticals, heavy metals, and industrial waste.

Ferrite nanomaterials such as hematite (α-Fe_2O_3), maghemite (γ- Fe_2O_3), and goethite (α-FeOOH) are very promising materials not only because of their low production cost but also because of their superior arsenic adsorption efficiency, stability, and resistance to arsenic reuse. Among them, α-Fe_2O_3 nanoparticles have been widely used for environmental protection, equipment manufacturing, biomedicine, chemical catalysis and other fields because of their stable structure and excellent performance. α-Fe_2O_3 nanoparticles exhibit good separation efficiency and cycling performance due to their superior magnetic properties (Zhao et al., 2023). Therefore, various investigations focused on methods for the adsorption and oxidation–reduction remediation of α-Fe_2O_3 have been widely conducted. Other studies have obtained results from mixed-phase (80:20%) α/γ-Fe_2O_3 catalysts, which are very promising for magnetically separating materials and are suitable candidates for dye-containing wastewater treatment applications (Magomedova et al., 2023).

Many methods for fabricating α-Fe_2O_3 nanoparticles, such as coprecipitation, microemulsion, arc-discharge, solvothermal, sono-chemical, microwave-assisted, chemical vapor deposition, combustion, laser pyrolysis, sol-gel and high-temperature decomposition of organic precursors, have been developed (Fouad et al., 2019; Ikram et al., 2022; Zhao et al., 2023). However, this method requires a large amount of energy during the sample preparation process. Other methods, such as electrochemical deposition and stepwise anodization, can produce α-Fe_2O_3 nanotube composites. For example, in the research of Li and Dong (2017). The Cu_2O@graphene@Fe_2O_3 nanotube composites were synthesized via a two-stage electrolysis method in which GO sheets were first deposited onto the Fe_2O_3 nanotubes, and then, the Cu_2O

nanoparticles were immobilized on the GO@ Fe_2O_3 in the same way. However, the shortcomings of this system are that poor dispersion and agglomeration easily occur in the sample. In research on the environment, Fe_2O_3 was obtained by calcining Prussian blue (PB) octahedral microcrystals at high temperatures. As a material used for the adsorption of organic pollutants in water, Fe_2O_3 has high efficiency because of its outstanding catalytic properties and structured pores. The Fe_2O_3 micromotors display excellent performance in water cleaning with high efficiency at low H_2O_2 concentrations. Fe_2O_3 micrometres can also move directionally, are easily recovered using magnets and are nontoxic (Xiang et al., 2019).

In this study, the process of making α-Fe_2O_3 nanoparticles encapsulated with PEG 6000 through the coprecipitation method was carried out. The coprecipitation method is more convenient in the process of synthesizing α-Fe_2O_3 nanoparticles, where the advantage of the coprecipitation method is the ability to produce samples with a highly homogeneous phase with a low process temperature and short synthesis duration. PEG 6000 was used to encapsulate the α-Fe_2O_3 nanoparticles to avoid aggregation. PEG 6000 has good thermal resistance, so it is not flammable and is not corrosive [14]. During the process of making α-Fe_2O_3 nanoparticles and capsulation, the process temperature was varied, namely, 60, 70, or 80°C. Furthermore, the phase, microstructure, density, and adsorption of Mn ions on the synthesized material were analyzed.

METHOD

α-Fe_2O_3 was synthesized via coprecipitation by mixing 10 grams of Fe iron sand and 77 ml of HCl. The mixed material was then stirred using a magnetic stirrer and a hot plate within 1 hour with a rotating speed of 1000 rpm at room temperature. After that, the stirred solution was filtered through filter paper for 1 hour. The chemical reaction equation that occurs can be seen in equation (1).

$$Fe_2O_3 + 6HCl \rightarrow 2FeCl_3 + 3H_2O \qquad (1)$$

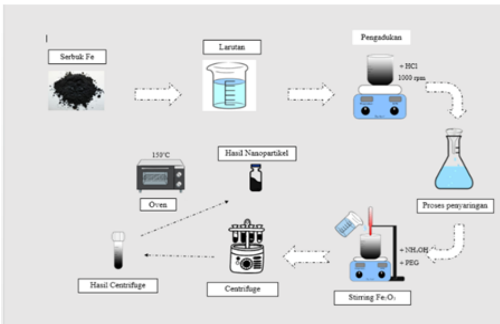

Figure 1. The synthesized process of α-Fe_2O_3.

Next, 5 grams of PEG 6000 were first dissolved in 10 ml of distilled water and stirred with a magnetic stirrer. After that, the process of titrating the PEG 6000 solution and ammonium hydroxide (NH4OH) solution (123.5 ml) simultaneously into a mixture of iron sand + HCl using a drop pipette while stirring with a magnetic stirrer with various process temperatures, namely, 60, 70, and 80°C. The solution was then left on a hot plate and stirred for 2 hours. Furthermore, the results of the titration process were washed 4 times with distilled water using a centrifuge to separate the precipitate formed. The precipitate was subsequently dried in an oven at 100°C for 24 hours.

The chemical reaction equation until the α-Fe_2O_3 precipitate is formed can be seen in equation 2 below:

$$2FeCl_3 + 6NH_4OH \rightarrow Fe_2O_3 + 3H_2O + 6NH_4Cl \quad (2)$$

The results of the synthesis were then analyzed for phase, microstructure, density, and adsorptivity using X-ray diffraction (XRD) (SmartLab Rigaku), scanning electron microscopy with energy-dispersive X-ray spectroscopy (SEM–EDS) (JEOL JSM-IT200), and pycnometer and atomic absorption spectroscopy (ASS) instruments.

RESULTS AND DISCUSSION

X-ray diffraction (XRD) analysis.

The XRD results are shown in Figure 2 with peaks in the (104) plane of the 2θ region, namely, 33.115°, 35.612°, and 54.005°, with varying temperatures, namely, 60, 70, and 80°C, respectively. The appearance of these peaks indicates that the α-Fe_2O_3 phase is well formed. The figure shows that the height of the main peak corresponds to the 80°C sample. At 80°C, samples with higher peaks have a higher purity of the α-Fe_2O_3 phase [15].

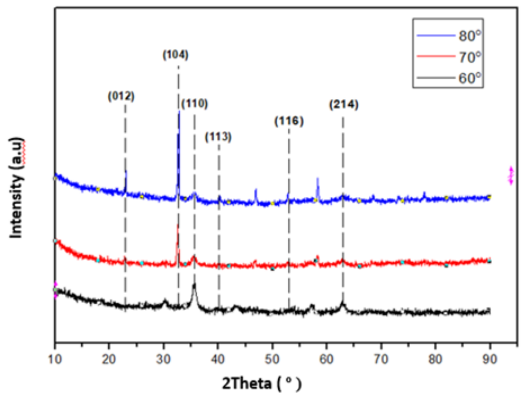

Figure 2. X-ray diffraction of α-Fe_2O_3.

A high degree of crystallization results from increasingly strong refraction and is determined by the number of phases formed. This was also obtained by (Lassoued et al., 2017a), who synthesized iron oxide nanoparticles through the precipitation process by varying the concentration of the basic ingredients for making Fe_2O_3 with the (012), (104), (110), (113), (116), and (214) crystal planes. Some peaks present in the sample are not characteristic of α-Fe_2O_3, suggesting the existence of contaminants. Moreover, the photos show that higher processing temperatures lead to increased strength of the peaks on the crystal plane (104). Increasing the processing temperature appeared to increase the quantity of the α-Fe_2O_3 phase.

The XRD data also show that the calculated size varies between the particle size growth and the process temperature variation used. The increase in particle size with increasing process temperature is due to the increase in density for nucleation in the synthesized α-Fe_2O_3 nanoparticles. Figure 2 also shows that narrower peaks and lower FWHM values occur with increasing process temperature.

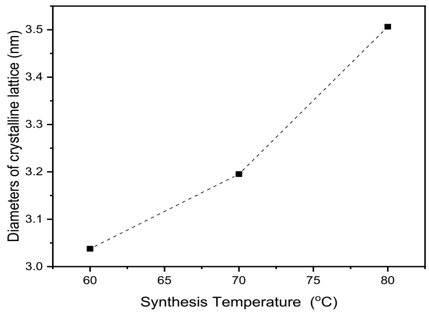

(a)

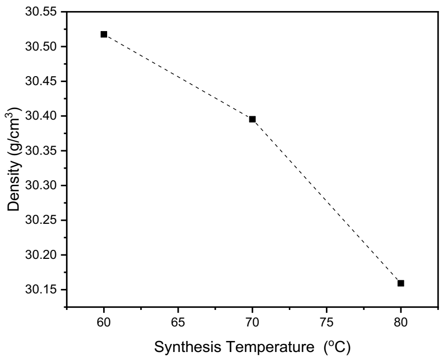

(b)

Figure 3. (a) Diameter crystallite of α-Fe_2O_3, **(b)** density of α-Fe_2O_3.

Figure 3a. shows the value of the crystallite diameter formed in the Fe_2O_3 phase. The data show that the formation of Fe_2O_3 nanoparticles reaches the nanometer scale, resulting in a crystallite diameter. The crystallite diameter range formed is 3–3.5 nm, where the greater the process temperature used, the greater the diameter of the crystallite formed. The increase in the crystal size is related to the increase in the annealing temperature, which can increase Oswald's maturation process (Van Westen and Groot, 2018). This is known as the diffusion process, where the particle size increases by eliminating small particles. Increasing the temperature in the reaction process increases the amount of thermal energy present in the nanoparticles, thus obtaining sufficient energy for diffusive motion, which increases the size of the crystallites (Setiadi et al., 2018)(Eldin et al., 2019).

Figure 3b. The density value at a temperature of 60°C, with a weight of 30.52 g/cm^{3,} is greater than that at the other temperatures; at 70°C, the density value is 30.39 g/cm^3, and the lowest density value is 80°C, with a weight of 30.16 g/cm^3. From this analysis, it can be concluded that the higher the temperature used is, the smaller the density value. This is due to the smaller diameter of the crystallites, which further increases the porosity (Lassoued et al., 2017b).

Scanning electron microscopy-energy-dispersive X-ray spectroscopy (SEM-EDX) analysis.

The SEM test results are shown in Figure 4. The image was obtained at a magnification of 10,000 times. The appearance of the Fe_2O_3 nanoparticle samples with the addition of PEG 6000 at 60°C is shown. Although it has been done with the addition of PEG-6000, agglomeration still occurs and is not homogeneous. This is because EG interacts with magnetic particles only through hydrogen bonds [20], but the Fe_2O_3 sample has succeeded since the particle size distribution is 62 nm. The particle size is shown in Figure 4. (b).

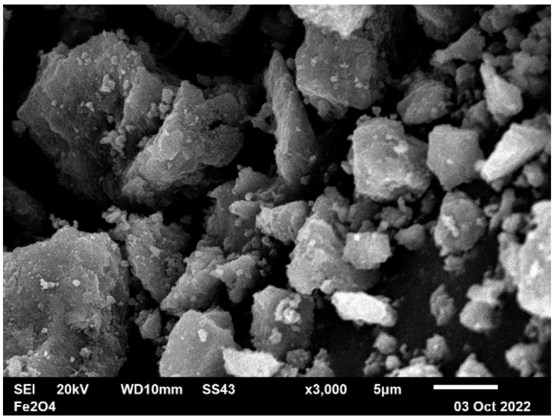

(a)

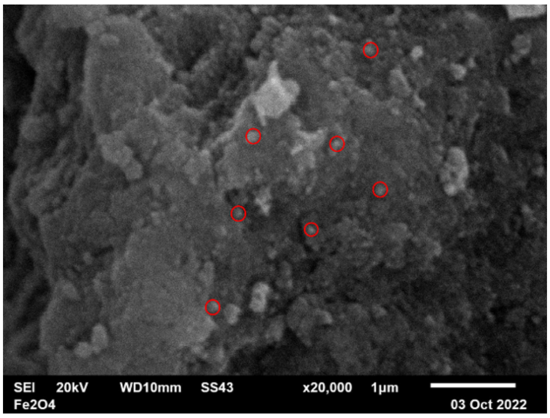

(b)

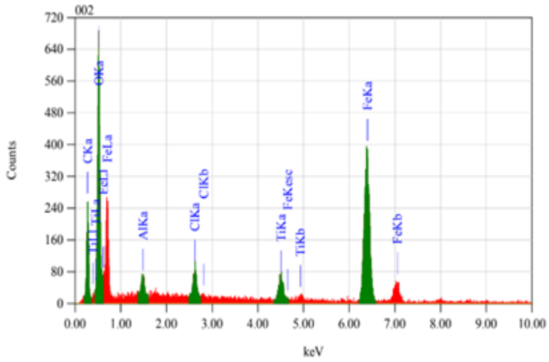

(c)

Figure 4. Micrograph of the synthesized α-Fe_2O_3 **(a)**, 5000x, **(b)** 20.000x, and **(c)** EDX result of α-Fe_2O_3.

Based on the SEM–EDS results, no PEG was found in the sample. The purpose of adding PEG 6000 is to prevent the agglomeration of the Fe_2O_3 powder, especially when it is used in adsorbent materials. This helps maintain the surface area of the material, ensuring that its ability to adsorb heavy Mn metals remains at an optimal level. However, the SEM results show that PEG-6000 does not react and only acts as a coating. In addition, the results of the SEM–EDS image above show that Fe_2O_3 synthesis produces Fe (ferrite) and O (oxygen) with high peaks, which are quite significant. This indicates that the growth of the nanoparticle phase formed significantly was the Fe_2O_3 phase. Although the EDS results still reveal the presence of impurities in the sample, some of the elements presents are titanium, Al (aluminum), and Cl (clorin).

Atomic Absorption Spectrometry (AAS)

Figure 5 shows the results of the AAS measurements, where the sample heated at 60°C has the lowest adsorption of Mn metal ions, namely, 191.39 μ/g. This is possibly due to the agglomeration in the sample so that the sample is not optimal for adsorbing Mn metal. The sample heated at 70°C, with a value of 2176.51 μ/g, has the highest content. This shows that the sample heated at 70°C is more effective at adsorbing Mn metal ions than the sample heated at 80°C, which adsorbs 1468.99 μ/g of Mn metal. This occurred because the 70°C sample has a relatively smaller particle size than the 80°C sample. The smaller the particle size is, the greater the surface area (Setiadi et al., 2018). In addition, the presence of a PEG 6000 layer on the surface of these nanoparticles also increases their stability and prevents oxidation at 70°C (Simbolon, 2018).

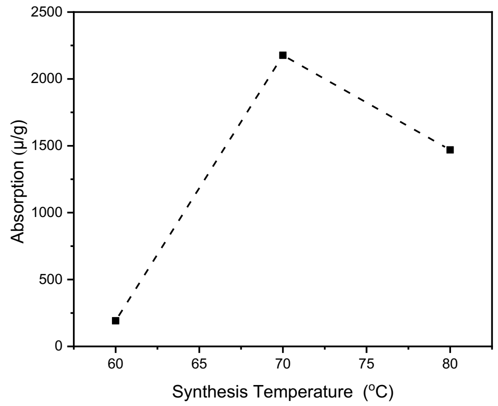

Figure 5. Atomic adsorption spectra of α-Fe_2O_3

CONCLUSION

The synthesis of Fe_2O_3 nanoparticles made from natural iron sand using the coprecipitation method was carried out. The physical properties of the XRD results for the Fe_2O_3 nanoparticles show that the particles crystallize well and that the crystal diameter is directly proportional to the temperature used during synthesis. Fe_2O_3 nanoparticles based on natural iron (Fe) sand contain other elements, such as Fe (ferrite), O (oxygen), Ti (titanium), Al (aluminum) and Cl (chlorine). The Fe_2O_3 nanoparticles have the smallest diameter at a temperature of 60°C, with an average diameter of 3.03760 nm. However, the SEM results show that the 60°C sample tends to agglomerate. The existence of temperature variations can affect the density value, where the higher the temperature used is, the smaller the density value obtained, and the adsorbent results obtained. The optimal conditions in this study were obtained at a process temperature of 70°C, which has the highest adsorbent value.

REFERENCES

Al-Hakkani, M.F., Gouda, G.A., Hassan, S.H.A., 2021. A review of green methods for phyto-fabrication of hematite (α-Fe2O3) nanoparticles and their characterization, properties, and applications. Heliyon 7, e05806. https://doi.org/10.1016/j.heliyon.2020.e05806

Brzóska, M.M., Gałażyn-Sidorczuk, M., Kozłowska, M., Smereczański, N.M., 2022. The Body Status of Manganese and Activity of This Element-Dependent Mitochondrial Superoxide Dismutase in a Rat Model of Human Exposure to Cadmium and Co-Administration of Aronia melanocarpa L. Extract. Nutrients 14. https://doi.org/10.3390/nu14224773

Eldin, D., Zhang, C., El-didamony, H., Yingnan, L., Daniel, T., Hussain, A., 2019. Results in Physics Improved size , morphology and crystallinity of hematite (α-Fe_2O_3) nanoparticles synthesized via the precipitation route using ferric sulfate precursor. Results Phys. 12, 1253–1261. https://doi.org/10.1016/j.rinp.2019.01.005

Fouad, D.E., Zhang, C., El-Didamony, H., Yingnan, L., Mekuria, T.D., Shah, A.H., 2019. Improved size, morphology and crystallinity of hematite (α-Fe_2O_3) nanoparticles synthesized via the precipitation route using ferric sulfate precursor. Results Phys. 12, 1253–1261. https://doi.org/10.1016/j.rinp.2019.01.005

Gulzar, Aanisa, Ayoub, N., Mir, J.F., Alanazi, A.M., Shah, M.A., Gulzar, Arif, 2022. In vitro and in vivo MRI imaging and photothermal therapeutic properties of Hematite (α-Fe2O3) Nanorods. J. Mater. Sci. Mater. Med. 33. https://doi.org/10.1007/s10856-021-06636-1

Huang, X., Luo, D., Zhao, D., Li, N., Xiao, T., Liu, J., Wei, L., Liu, Y., Liu, L., Liu, G., 2019. Distribution, source and risk assessment of heavy metal(oid)s in water, sediments, and corbicula fluminea of Xijiang River, China. Int. J. Environ. Res. Public Health 16. https://doi.org/10.3390/ijerph16101823

Ikram, H., Al Rashid, A., Koç, M., 2022. Synthesis and characterization of hematite (α-Fe_2O_3) reinforced polylactic acid (PLA) nanocomposites for biomedical applications. Compos. Part C Open Access 9, 100331. https://doi.org/10.1016/j.jcomc.2022.100331

Jiang, X., Teng, A., Xu, W., Liu, X., 2014. Distribution and pollution assessment of heavy metals in surface sediments in the Yellow Sea. Mar. Pollut. Bull. 83, 366–375. https://doi.org/10.1016/j.marpolbul.2014.03.020

Lassoued, A., Dkhil, B., Gadri, A., Ammar, S., 2017a. Control of the shape and size of iron oxide (α-Fe2O3) nanoparticles synthesized through the chemical precipitation method. Results Phys. 7, 3007–3015. https://doi.org/10.1016/j.rinp.2017.07.066

Lassoued, A., Dkhil, B., Gadri, A., Ammar, S., 2017b. Control of the shape and size of iron oxide (α-Fe2O3) nanoparticles synthesized through the chemical precipitation method. Results Phys. 7, 3007–3015. https://doi.org/10.1016/j.rinp.2017.07.066

Li, F., Dong, B., 2017. Construction of novel Z-scheme Cu2O/graphene/α-Fe2O3 nanotube arrays composite for enhanced photocatalytic activity. Ceram. Int. 43, 16007–16012. https://doi.org/10.1016/j.ceramint.2017.08.021

Magomedova, A., Isaev, A., Orudzhev, F., Sobola, D., Murtazali, R., Rabadanova, A., Shabanov, N.S., Zhu, M., Emirov, R., Gadzhimagomedov, S., Alikhanov, N., Kasinathan, K., 2023. Photo-Fenton-like Oxidation of Rhodamine B 1–13.

Rezaei, M., Kafaei, R., Mahmoodi, M., Sanati, A.M., Vakilabadi, D.R., Arfaeinia, H., Dobaradaran, S., Sorial, G.A., Ramavandi, B., Boffito, D.C., 2021. Heavy metals concentration in mangrove tissues and associated sediments and seawater from the north coast of Persian Gulf, Iran: Ecological and health risk assessment. Environ. Nanotechnology, Monit. Manag. 15, 100456. https://doi.org/10.1016/j.enmm.2021.100456

Riseberg, E., Chui, K., James, K.A., Melamed, R., Alderete, T.L., Corlin, L., 2022. A Longitudinal Study of Exposure to Manganese and Incidence of Metabolic Syndrome. Nutrients 14, 1–14. https://doi.org/10.3390/nu14204271

Setiadi, E.A., Yunus, M., Nababan, N., Simbolon, S., Kurniawan, C., Humaidi, S., Sebayang, P., Ginting, M., 2018. The effect of temperature on synthesis of MgFe2O4 based on natural iron sand by Co-precipitation method as adsorbent Pb ion. J. Phys. Conf. Ser. 985, 0–5. https://doi.org/10.1088/1742-6596/985/1/012046

Simbolon, S., 2018. Efek Sonikasi Terhadap Proses Pembentukan Nanopartikel Fe3O4 Yang Dimodifikasi Dengan Peg-6000. J. Tek. Mesin Cakram 1, 29. https://doi.org/10.32493/jtc.v1i1.1345

Van Westen, T., Groot, R.D., 2018. Effect of Temperature Cycling on Ostwald Ripening. Cryst. Growth Des. 18, 4952–4962. https://doi.org/10.1021/acs.cgd.8b00267

Xiang, R., Duan, Y., Tong, C., Peng, L., Wang, J., Shah, S.S.A., Najam, T., Huang, X., Wei, Z., 2019. Self-standing FeCo Prussian blue analogue derived FeCo/C and FeCoP/C nanosheet arrays for cost-effective electrocatalytic water splitting. Electrochim. Acta 302, 45–55. https://doi.org/10.1016/j.electacta.2019.01.170

Yi, Y., Tang, C., Yi, T., Yang, Z., Zhang, S., 2017. Health risk assessment of heavy metals in fish and accumulation patterns in food web in the upper Yangtze River, China. Ecotoxicol. Environ. Saf. 145, 295–302. https://doi.org/10.1016/j.ecoenv.2017.07.022

Zhao, Z., Li, S., Zhang, Y., Guo, P., Zhao, X., Li, Y., 2023. Repurposing of steel rolling sludge: Solvent-free preparation of α-Fe2O3 nanoparticles and its application for As(III/V)-containing wastewater treatment. J. Environ. Manage. 342, 118286. https://doi.org/10.1016/J.JENVMAN.2023.118286